Vibrational Spectroscopy of Conducting Polymers

Yukio Furukawa

Reproduced from:

Handbook of Vibrational Spectroscopy

John M. Chalmers and Peter R. Griffiths (Editors)

Vibrational Spectroscopy of Conducting Polymers

Yukio Furukawa
Waseda University, Tokyo, Japan

1 INTRODUCTION

A new field of materials science resulted from the discovery of organic polymers having conjugated π-electrons: polyacetylene, polythiophene, poly(*p*-phenylene), poly(*p*-phenylenevinylene), etc.[1–3] The chemical structures of the conjugated polymers are shown in Figure 1. These conjugated polymers are organic semiconductors whose band gaps are typically in the range from 1 to 3 eV. A conjugated polymer can be doped chemically with an electron acceptor such as halogens, AsF_5, and $FeCl_3$ or an electron donor such as alkali metals. The chemical doping is performed by exposing a polymer film in various ways to an acceptor or a donor. The main process of doping is redox reaction between polymer chains and acceptors or donors. Upon acceptor doping (p-type doping), an ionic complex consisting of multiply oxidized (positively charged) polymer chains and counter anions (e.g. I_3^-, AsF_6^-) is formed. Counter anions are generated by reduction of acceptors. In the case of donor doping (n-type doping), an ionic complex consisting of multiply reduced (negatively charged) polymer chains and counter cations (e.g. Na^+, K^+) is formed. Counter cations are generated by oxidation of donors. The electrical conductivity of the polymer increases with increasing content of the dopant. In a heavily doped state, the polymer shows metallic properties. Since the electrical conductivity (i.e. the Fermi level) of a conjugated polymer can be controlled by the content of a dopant, conjugated polymers can be used as organic semiconductors or metals. Doping also can be performed electrochemically. It has been demonstrated that conjugated polymers can be used for field-effect transistors,[4,5] photovoltaic cells (solar cells),[6] and light-emitting diodes,[7,8] as organic semiconductors. The properties of conjugated polymers have been interpreted by new concepts of elementary electronic excitations such as solitons,[9] polarons,[10–12] and bipolarons.[11–13] Since they can move along a polymer chain or hop between chains, they are also called quasi-particles. Charged excitations such as charged solitons, polarons, and bipolarons are considered to be charge carriers. Charge carriers can be generated by light irradiation and injection in junction structures. These new techniques in carrier generation are used for transistors, light-emitting diodes, photovoltaic cells, etc.

Conjugated polymers can be classified into degenerate and nondegenerate polymers, according to the degeneracy of the ground states. The prototype of degenerate polymers is *trans*-polyacetylene, which has a simple structure with alternating C=C and C–C bonds. The energy curve of *trans*-polyacetylene has two equal minima, where the alternating C=C and C–C bonds are reversed. However, a nondegenerate polymer has no two identical structures in the ground state. Most conjugated polymers belong to this class. The types of elementary excitations depend on the degeneracy of ground states. When an electron is removed from a nondegenerate polymer such as polythiophene, charge $+e$ and spin 1/2 are localized over several repeating units with structural changes, as shown schematically in Figure 2(a). This is called a positive polaron. Since a positive polaron has charge $+e$ and spin 1/2, it corresponds to a radical cation in chemical terminology. When another electron is removed from the positive polaron, charge $+2e$ is localized over several units, as shown in Figure 2(b). This species is called a positive bipolaron, which has charge $+2e$ and no spin. Bipolarons are spinless carriers. A positive bipolaron corresponds to a dication in chemical terminology. If a bipolaron is unstable, two polarons are formed, as shown in Figure 2(c). In the case of donor doping, a negative polaron and a negative bipolaron can be formed. In a

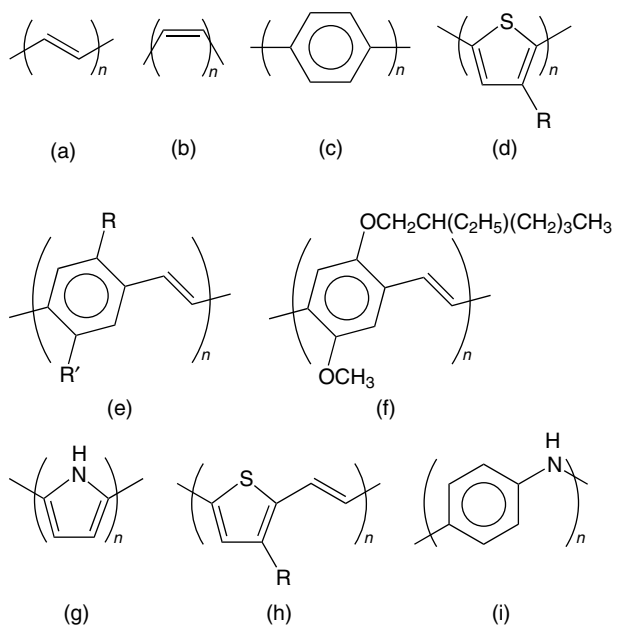

Figure 1. Chemical structures of conjugated polymers: (a) *trans*-polyacetylene; (b) *cis*-polyacetylene; (c) poly(*p*-phenylene); (d) polythiophenes (R: H, C_6H_{13}, C_8H_{17}, etc.); (e) poly(*p*-phenylenevinylene)s (R, R′: H, OCH_3, OC_6H_{13}, C_8H_{17}, etc.); (f) poly(2-methoxy-5-(2′-ethylhexyloxy)-*p*-phenylenevinylene) (MEH-PPV); (g) polypyrrole; (h) poly(2,5-thienylenevinylene)s (R, R′: OCH_3, OC_6H_{13}, etc.); (i) polyaniline (emeraldine base form).

degenerate polymer such as *trans*-polyacetylene, solitons can be formed. Solitons are classified into neutral, positive, and negative types according to their charges. A neutral soliton has no charge and spin 1/2 (Figure 2d). A positive soliton has charge $+e$ and no spin (Figure 2e). A negative soliton has charge $-e$ and no spin. Charged solitons are spinless carriers. A neutral soliton, a positive soliton, and a negative soliton correspond to the neutral radical, the cation, and the anion of a linear *trans*-oligoene with an odd number of carbon atoms, respectively. Although the charge and/or spin are depicted as being localized on one carbon atom in Figure 2(a–e), it should be noted that they extend over several rings with structural changes in real polymers. Elementary excitations in conjugated polymers are listed in Table 1, together with the corresponding chemical terms. Since these excitations are associated with structural changes, they are also called self-localized excitations.

Actual samples of conjugated polymers have more or less sp^3 defects and a distribution of conjugation length. The structures of neutral conjugated polymers (such as conformations, configurations, conjugation length, defects, etc.) can be obtained by infrared (IR) and Raman spectroscopy. Spectroscopic studies of well-defined oligomers are useful for a better understanding of the Raman and IR spectra of pristine polymers. Studies on vibrational spectra of pristine conjugated polymers and doping- and photo-induced IR absorption spectra have been reviewed previously.[14–18] Recently, electronic and vibrational spectra associated with the charge carriers generated by doping have been discussed.[19–21] In this article, we will focus our attention on the Raman and IR studies of charge carriers. The charged species of oligomers are models of the charge carriers, polarons, bipolarons, and charged solitons, in conjugated polymers. Thus the studies of the charged species of oligomers are useful for explaining the Raman and IR spectra originating from carriers. In this article, we will mention the vibrational spectra of pristine polymers briefly,

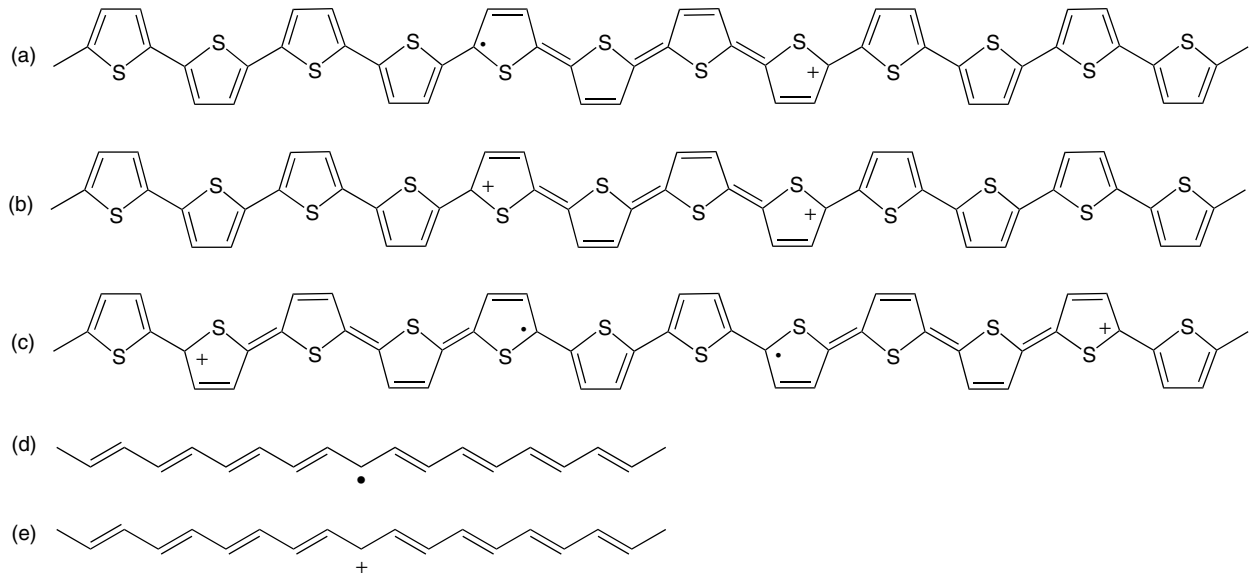

Figure 2. Schematic structures of elementary excitations: (a) a positive polaron; (b) a positive bipolaron; (c) two positive polarons; (d) a neutral soliton; (e) a positive soliton.

Table 1. Elementary excitations in conjugated polymers and chemical terminology.

Elementary excitation	Chemical term	Charge	Spin
Positive polaron	Radical cation	$+e$	1/2
Negative polaron	Radical anion	$-e$	1/2
Positive bipolaron	Closed-shell dication	$+2e$	0
Negative bipolaron	Closed-shell dianion	$-2e$	0
Neutral soliton	Neutral radical	0	1/2
Positive soliton	Cation	$+e$	0
Negative soliton	Anion	$-e$	0
Singlet exciton	S_1	0	0
Triplet exciton	T_1	0	1

and describe the Raman and IR studies on carriers generated by chemical doping, light irradiation, and injection.

2 INFRARED AND RAMAN SPECTRA OF PRISTINE POLYMERS

Totally symmetric bands are dominant in the observed Raman spectra of pristine conjugated polymers in most cases, and they reflect effective conjugation length of the polymer chains. In the IR spectra of pristine conjugated polymers, the CH out-of-plane bending vibrations, which are markers of geometrical isomerism or substituent positions of benzene rings or heterocycles, are strongly observed. The Raman and IR spectra of several representative polymers are shown in Figures 3 and 4, respectively. The vibrational spectra of *trans*-polyacetylene, *cis*-polyacetylene, polythiophene, poly(*p*-phenylene), poly(*p*-phenylenevinylene), etc. have been assigned on the basis of infinite planar structures for the first approximation. The point groups and vibrational irreducible representation at the zone center ($k = 0$) for each conjugated polymer are listed in Table 2.

The Raman and IR spectra of *trans*-polyacetylene are shown in Figures 3(a) and 4(a), respectively. The Raman spectrum is taken with the 1064-nm laser line. A planar infinite *trans*-polyacetylene chain is isomorphous to the point group C_{2h}. There are five Raman-active modes including one CH stretching and three IR-active modes including one CH stretching. The assignments of the observed bands have been made on the basis of the wavenumber shifts on isotope substitutions and normal coordinate calculations.[22–27] The Raman bands observed at 1458, 1294, and 1068 cm^{-1} are assigned to the $\nu_2(a_g)$, $\nu_3(a_g)$, and $\nu_4(a_g)$ modes. The 881-cm^{-1} Raman band is assigned to the $\nu_6(b_g)$ mode. The IR band observed at 1251 cm^{-1} is assigned to the $\nu_8(b_u)$ mode. The intense IR band at 1012 cm^{-1} is characteristic of the CH out-of-plane wagging ($\nu_5(a_u)$) associated with *trans*-CH=CH groups, whereas

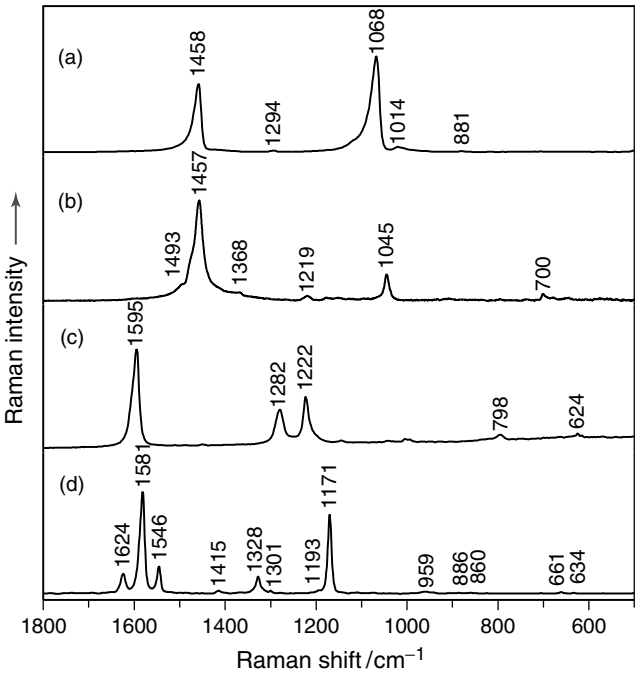

Figure 3. Raman spectra of conjugated polymers: (a) *trans*-polyacetylene; (b) polythiophene; (c) poly(*p*-phenylene); (d) poly(*p*-phenylenevinylene). Excitation wavelength is 1064 nm.

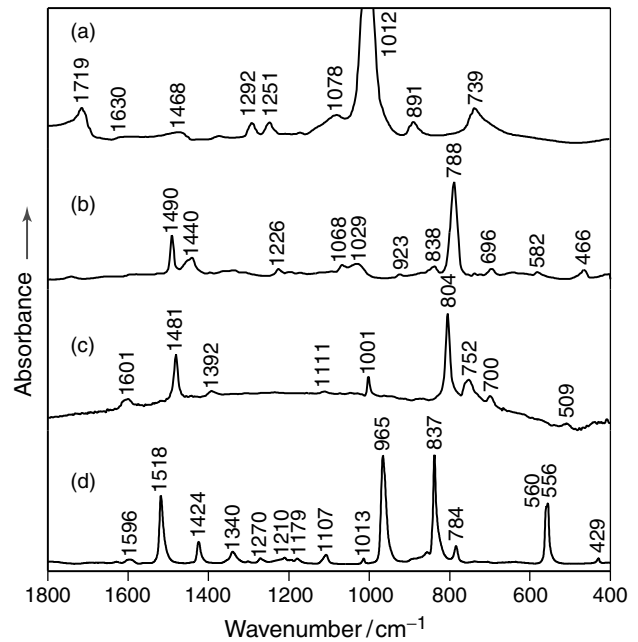

Figure 4. IR spectra of conjugated polymers: (a) *trans*-polyacetylene; (b) polythiophene; (c) poly(*p*-phenylene); (d) poly(*p*-phenylenevinylene).

the corresponding band of *cis*-CH=CH groups is observed at 740 cm^{-1}. The assignments of weak bands are given in Takeuchi *et al.*[26] and Hirata *et al.*[27] The Raman spectra of *trans*-polyacetylene have been explained by the effective conjugation coordinate (ECC) theory proposed

Table 2. Point groups and vibrational representations.

Polymer	Point group	Representation[a]
trans-Polyacetylene	C_{2h}	$4a_g(R) + a_u(IR) + b_g(R) + 2b_u(IR)$
Polythiophene[b]	D_{2h}	$7a_g(R) + 3a_u + 7b_{1g}(R) + 3b_{1u}(IR) + 3b_{2g}(R) + 6b_{2u}(IR) + 3b_{3g}(R) + 6b_{3u}(IR)$
Poly(*p*-phenylene)[b]	D_{2h}	$5a_g(R) + 2a_u + 5b_{1g}(R) + 2b_{1u}(IR) + 3b_{2g}(R) + 4b_{2u}(IR) + b_{3g}(R) + 4b_{3u}(IR)$
Poly(*p*-phenylenevinylene)	C_{2h}	$14a_g(R) + 6a_u(IR) + 6b_g(R) + 12b_u(IR)$

[a]R and IR denote Raman- and IR-active vibrations, respectively. The a_g and b_u modes are in-plane vibrations, and the a_u and b_g modes are out-of-plane vibrations. The a_g, b_{1g}, b_{2u} and b_{3u} modes are in-plane vibrations, and the a_u, b_{1u}, b_{2g} and b_{3g} modes are out-of-plane vibrations.
[b]The xy plane is taken in the polymer plane (x-axis along the polymer chain) and the z axis perpendicular to the polymer plane.

by Castiglioni *et al.*[28] Their theory has been successfully applied to other conjugated polymers.[16,18] Their theory is a molecular spectroscopy version of the amplitude mode theory.[29,30] According to these theories, the vibrational modes that induce oscillations in bond alternation have strong Raman intensities. The $\nu_2(a_g)$ and $\nu_4(a_g)$ vibrations modulate strongly bond alternation: antisymmetric stretching of C=C and C–C bonds. It is well known that the ν_2 and ν_4 Raman bands of *trans*-polyacetylene in Figure 3(a) show changes in wavenumber and/or bandshape with the excitation of various wavelengths. These observations reflect the coexistence of the segments having various conjugation lengths in a *trans*-polyacetylene film.

An important problem remaining to be solved in the vibrational spectra of *trans*-polyacetylene is the assignment of the Raman band observed at 1014 cm^{-1}. This band has been assigned to the CH out-of-plane wagging mode that is IR active and Raman inactive on the basis of the wavenumber shift on ^{13}C-substitution.[26] The appearance of the Raman-inactive mode in the Raman spectrum can be explained by the reduction of symmetry due to the distortion of polyacetylene chains. Recently, helical polyacetylene has been synthesized by using chiral nematic liquid crystal solvents.[31] Probably, *trans*-polyacetylene films prepared by the previous method are the racemic mixtures of helical chains.

The Raman and IR spectra of polythiophene are shown in Figures 3(b) and 4(b), respectively. The observed bands have been explained by assuming a coplanar *s-trans* infinite structure (D_{2h}).[32–37] In reference 37, the Raman bands observed at 1457, 1368, 1219, 1045, and 700 cm^{-1} are assigned to the $\nu_2(a_g)$, $\nu_3(a_g)$, $\nu_4(a_g)$, $\nu_5(a_g)$, and $\nu_6(a_g)$ modes, respectively. The 1493-cm^{-1} band is assigned to the $\nu_{12}(b_{1g})$ mode. However, different assignments are proposed for the Raman bands observed at 1493 and 1368 cm^{-1}. Navarrete and Zerbi[35] assigned the 1493-cm^{-1} band to a totally symmetric fundamental band instead of the 1368-cm^{-1} band. The marker bands of distorted structures, conjugation length, etc. are reviewed in Harada and Furukawa.[15] The 786-cm^{-1} IR band is assigned to the CH out-of-plane wagging $\nu_{18}(b_{1u})$ of 2,5-disubstituted thiophene rings and the 695-cm^{-1} band to the CH out-of-plane wagging of terminal 2-monosubstituted thiophene rings. Thus the intensity ratio of these bands can be used as a marker of the degree of polymerization. The 466-cm^{-1} IR band is also assigned to the out-of-plane bending vibration $\nu_{19}(b_{1u})$. The 1490- and 1440-cm^{-1} IR bands are assigned to the C=C antisymmetric stretching $\nu_{34}(b_{3u})$ and symmetric stretching $\nu_{25}(b_{2u})$, respectively. The complete assignments of the observed IR bands have not been made yet.

The Raman and IR spectra of poly(*p*-phenylene) are shown in Figures 3(c) and 4(c), respectively. These spectra have been analyzed by a coplanar infinite polymer structure (D_{2h}). Major Raman and IR bands have been assigned on the basis of the wavenumber shifts on isotope substitutions and normal coordinate calculations.[21,38–41] The Raman bands observed at 1595, 1282, 1222, 798, and 624 cm^{-1} are assigned to $\nu_2(a_g)$, $\nu_3(a_g)$, $\nu_4(a_g)$, $\nu_5(a_g)$, and $\nu_{11}(b_{1g})$, respectively. The IR band observed at 804 cm^{-1} is assigned to the CH out-of-plane wagging of para-disubstituted benzene rings $\nu_{13}(b_{1u})$. The IR bands at 752 and 700 cm^{-1} are due to CH out-of-plane wagging of terminal phenyl rings. The observation of these two bands suggests that the degree of polymerization is rather small.

The Raman and IR spectra of poly(*p*-phenylenevinylene) are shown in Figures 3(d) and 4(d), respectively. These spectra have been analyzed by a coplanar infinite polymer structure (C_{2h}).[42,43] There are fourteen a_g modes including three CH stretchings. The Raman bands observed at 1624, 1581, 1546, 1328, 1301, 1193, 1171, 886, 661, 634, and 328 cm^{-1} are assigned to the in-plane a_g fundamental modes. There are twelve b_u modes including three CH stretchings. The IR bands observed at 1518, 1424, 1340, 1270, 1179, 1107, 1013, 784, and 429 cm^{-1} are assigned to the in-plane b_u fundamental modes. The 965-cm^{-1} IR band is assigned to the CH out-of-plane wagging of the *trans* vinylene groups. No band due to *cis* vinylene group is observed. The 837-cm^{-1} band is assigned to the in-phase CH out-of-plane wagging of para-disubstituted benzene rings. The 556-cm^{-1} band is also assigned to an out-of-plane vibration. The weak Raman band observed at 959 cm^{-1} is probably assigned to the CH out-of-plane

wagging that is IR active and Raman inactive under local C_{2h} symmetry of the *trans* planar structure. The observation of this mode in the Raman spectrum possibly reflects the distortion of the vinylene group from the *trans* planar form.

3 RAMAN SPECTRA OF DOPED POLYMERS

Most pristine conjugated polymers show the $\pi-\pi^*$ electronic absorptions in the region from ultraviolet to visible. Upon doping, new absorption bands associated with the sub-gap bands of elementary excitations appear in the region from visible to IR. Thus, the structures of doped polymers (elementary excitations generated by doping) can be studied by resonance Raman spectroscopy with a wide range of excitation wavelength from visible to IR.[44] The longest excitation wavelength used so far is 1320 nm. Clear conclusions were not obtained in previous Raman studies on doped states, because it is difficult to assign the observed Raman bands. A positive polaron (charge $+e$, spin 1/2) and a negative polaron (charge $-e$, spin 1/2) correspond to the radical cation and the radical anion of an oligomer, respectively. A positive bipolaron (charge $+2e$, spin 0) and a negative bipolaron (charge $-2e$, spin 0) correspond to the closed-shell dication and the closed-shell dianion of an oligomer, respectively. Thus, marker bands for identifying polarons and bipolarons can be obtained from the studies of the radical ions and the divalent ions of oligomers. Thus studies of charged oligomers are very important. Recently, the Raman spectra of the charged species of oligomers have been studied extensively. The chemical structures of the oligomers described in this article are shown in Figure 5.

Before going to the Raman studies of doped polymers, it is useful to describe the electronic states of charge carriers in conjugated polymers.[20,45] The schematic electronic structures of carriers are shown in Figure 6. Although excitonic effect or electron correlation plays an important role in the optical properties of conjugated polymers and oligomers, we will use a one-electron picture because of its simplicity. The band structure of a neutral polymer is shown in Figure 6(a). For a polaron or a bipolaron, two localized electronic levels, bonding and antibonding, are formed symmetrically with respect to the gap center at $-\omega_0$ and $+\omega_0$, respectively, as shown in Figure 6(b–e). The positions of the localized electronic levels, i.e. $\pm\omega_0$, depend on the extent of the structural changes associated with the polarons and the bipolarons. When a positive polaron is formed, one electron is removed from the $-\omega_0$ level. Thus a positive polaron has two sub-gap transitions, P_1 and P_2 (Figure 6b). When a negative polaron is formed, one electron is added to the $+\omega_0$ level. Thus a negative polaron also has two sub-gap transitions, P_1 and P_2 (Figure 6c). When a positive bipolaron is formed, two electrons are removed from the $-\omega_0$ level. Thus a positive bipolaron has a single sub-gap transition BP_1 (Figure 6d). When a negative bipolaron is formed, two electrons are added to the $+\omega_0$ level. Thus a negative bipolaron has a single sub-gap transition BP_1 (Figure 6e). For a positive and a negative soliton, S, a nonbonding level is formed in the center of the band gap. Thus, a single sub-gap absorption is expected to be observed at the middle of the band edge of the neutral polymer as shown in Figure 6(g) and (h).

3.1 Doped polyacetylene

The Raman spectra of doped polyacetylene have been measured with excitation of various wavelengths.[23,46–50] The Raman spectra of *trans*-polyacetylene and heavily Na-doped *trans*-polyacetylene with 1320-nm excitation[50] are shown in Figure 7(a) and (b), respectively. The electronic absorption band of heavily Na-doped *trans*-polyacetylene appears from visible to IR, whereas a band that has peaked

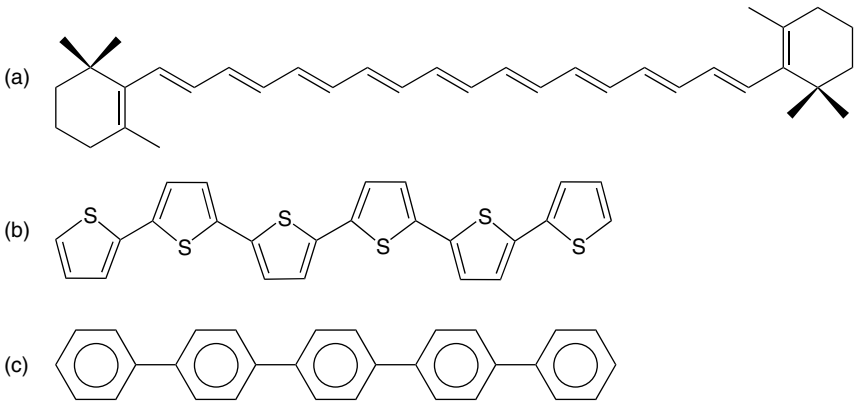

Figure 5. Chemical structures of (a) 19,19′,20,20′-tetranor-β,β-carotene (TNBC), (b) α-sexithiophene, and (c) *p*-quinquephenyl.

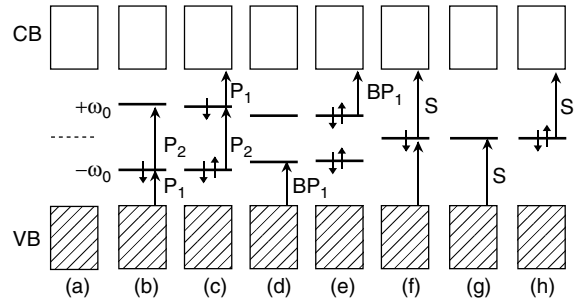

Figure 6. Schematic electronic structures of elementary excitations: (a) neutral polymer; (b) positive polaron; (c) negative polaron; (d) positive bipolaron; (e) negative bipolaron; (f) neutral soliton; (g) positive soliton; (h) negative soliton.

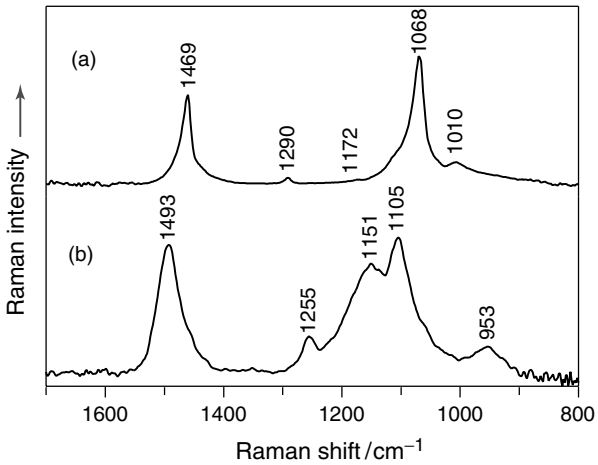

Figure 7. Raman spectra of (a) *trans*-polyacetylene and (b) heavily Na-doped *trans*-polyacetylene ($CHNa_{0.14}$). Excitation wavelengths are 1320 nm.

at 1.83 eV, which is due to neutral *trans*-polyacetylene, disappears completely. Since the excitation wavelength 1320 nm locates within the doping-induced absorption, the 1320-nm excited Raman spectrum mainly arises from new structures generated by Na doping. It is expected that negative polarons or negative solitons can be formed by Na doping. The ν_2 band of *trans*-polyacetylene shows an upward shift from 1469 to 1493 cm^{-1} upon Na doping. The ν_3 band shows a downward shift from 1290 to 1255 cm^{-1} upon Na doping. The ν_4 band also shows an upward shift from 1068 to 1105 cm^{-1} upon Na doping. A broad strong band is observed at 1151 cm^{-1}, which corresponds to the 1172-cm^{-1} band of pristine *trans*-polyacetylene. These spectral changes will be compared with those of model compounds.

The Raman spectra of the neutral species, the radical anion, and the dianion of TNBC are shown in Figure 8(a).[51] The radical anion corresponds to a negative polaron, whereas the dianion corresponds to two negative solitons. The radical anion of TNBC has an intense absorption at 1.46 eV (849 nm) and a weak band at 1.00 eV (1240 nm), whereas the neutral TNBC has a band peaked at

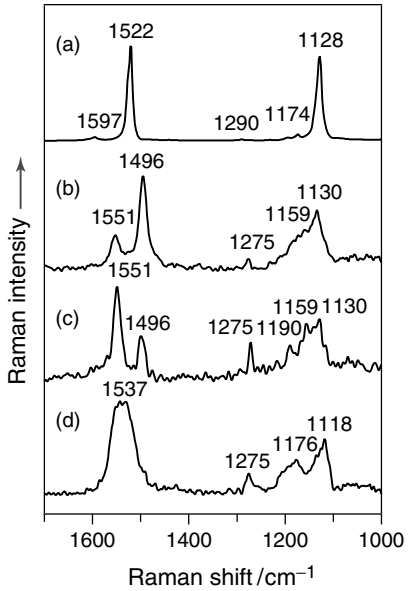

Figure 8. Raman spectra of the various oxidation states of TNBC: (a) neutral species; (b) and (c) radical anion; (d) dianion. Excitation wavelengths used in (a), (b), (c), and (d) are 1064, 1064, 1320, and 1064 nm, respectively. (a) Solid; (b), (c), and (d), tetrahydrofuran (THF) solutions. The bands of THF and background are subtracted in (b), (c), and (d).

2.82 eV (440 nm). An intense fluorescence background has prevented us from observing the rigorous resonance Raman spectra of the radical anion excited at either 753 nm (1.65 eV) or 781 nm (1.59 eV) within the 1.46-eV electronic absorption band. However, the Raman spectra of the radical anion have been obtained with excitation at either 1064 nm (1.17 eV) or 1320 nm (0.94 eV). The 1551- and 1496-cm^{-1} bands (C=C stretchings) of the radical anion correspond to the 1597- and 1522-cm^{-1} bands of neutral TNBC, respectively. The lower wavenumber shift of each band reflects a decrease in the C=C bond order. The 1290-cm^{-1} band of TNBC downshifts to 1275 cm^{-1} for the radical anion. The 1128-cm^{-1} band upshifts to 1130 cm^{-1}. This small upshift seems to be the result of strong mixing between the C–C and C=C stretches. The intensity of each of the 1551-, 1275-, 1190-, and 1159-cm^{-1} bands in the 1320-nm excited spectrum is stronger than that in the 1064-nm excited spectrum.

The dianion of TNBC has an intense absorption at 1.59 eV (780 nm). It was not possible to observe the resonance Raman spectrum of the dianion with the 632.8- or 753-nm excitation line, because of the presence of an intense fluorescence background. However, a pre-resonant Raman spectrum of the dianion has been observed with the 1064-nm excitation line (Figure 8d). The 1537-cm^{-1} broad band of the dianion corresponds to the 1522-cm^{-1} band of neutral TNBC. This 15-cm^{-1} upshift observed for the dianion cannot be explained by a simple consideration

of the bond order of the C=C bonds. This upshift may originate from large structural changes on going from the neutral TNBC to the anion. According to the *ab initio* molecular orbital calculations of 1,3,5,7,9-decapentaene,[52] bond alternation is reversed in the middle of the chain. The 1275-cm^{-1} band of the dianion corresponds to the 1290-cm^{-1} band of the neutral species. The low wavenumber position of the ν_3 band is a marker of negatively charged polyenes. The 1118-cm^{-1} band of the dianion corresponds to the 1128-cm^{-1} band of the neutral species. This 10-cm^{-1} downshift also may reflect the inversion of the bond alternation.

It seems that the spectral changes observed for *trans*-polyacetylene upon Na doping are similar to those observed for TNBC on going from the neutral species to the dianion (two negative solitons). However, further experimental and theoretical studies on the charged species of polyenes are requisite for a complete analysis of the Raman spectra of Na-doped *trans*-polyacetylene.

3.2 Doped polythiophene

The as-polymerized BF_4^--doped polythiophene prepared by an electrochemical method has two broad absorption bands peaked at 1.68 and 0.73 eV (738 and 1700 nm).[53] In a nondegenerate conjugated polymer such as polythiophene, polarons or bipolarons are expected to be formed by doping. The observed two bands are attributable to positive polarons, because a polaron gives rise to the two sub-gap electronic absorption bands, whereas a positive bipolaron gives rise to a single band. The Raman spectra of an as-polymerized BF_4^--doped polythiophene film excited at 753 and 1064 nm are shown in Figure 9(a) and (b), respectively.[53] The excitation lines, 753 and 1065 nm, locate within the doping-induced electronic absorptions. The observed Raman spectra are different from that of pristine polythiophene. These spectra are attributable to the charge carriers generated by doping.

The radical cation and the dication of α-sexithiophene correspond to a positive polaron and a positive bipolaron, respectively. Thus, the Raman spectra of the radical cation and the dication are useful for determining the types of elementary excitations generated by doping. The Raman spectra of the neutral species, the radical cation, and the dication of α-sexithiophene are shown in Figure 10.[53] The 753- and 1064-nm excited Raman spectra are quite similar to the spectrum of the radical cation, but different from that of the dication. This indicates that positive polarons are generated by doping in the BF_4^--doped polythiophene film, which is consistent with the conclusion drawn by the electronic absorption study. The normal coordinate

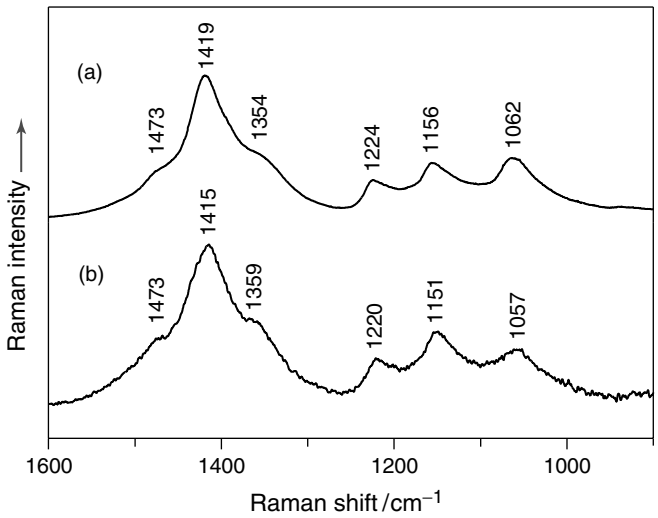

Figure 9. Raman spectra of a BF_4^--doped polythiophene film. Excitation wavelengths are 753 and 1064 nm for (a) and (b), respectively.

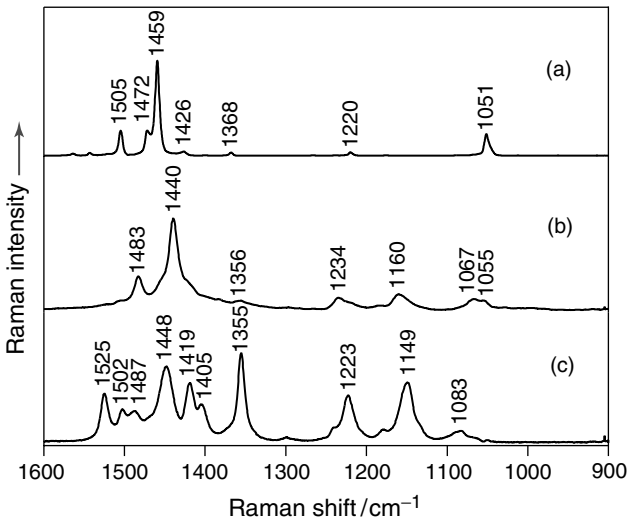

Figure 10. Raman spectra of the various oxidation states of α-sexithiophene: (a) neutral species; (b) radical cation; (c) dication. Excitation wavelengths used in (a), (b), and (c) are 1064, 781, and 781 nm, respectively. (a) Solid; (b) CH_2Cl_2 solution; (c) CD_2Cl_2 solution. The bands of the solvents and backgrounds are subtracted in (b) and (c).

calculations of the radical cations and the dications of oligothiophenes have been made by means of the *ab initio* molecular orbital method and density functional theory method.[54–56] The strongest band at 1440 cm^{-1} is assigned to the mixture of the C=C and C–C stretchings.

In the as-polymerized BF_4^--doped polythiophene, only polarons exist. However, stabilities of polarons and bipolarons depend on the dopant concentration. Apperloo *et al.*[57] have shown that bipolarons are formed for heavily doped poly(3-alkylthiophene) in a solution by using electronic absorption spectroscopy.

3.3 Doped poly(*p*-phenylene)

The Raman spectra of Na-doped poly(*p*-phenylene) depend on the excitation wavelength.[58] The Raman spectra excited at 514.5 and 1064 nm are shown in Figure 11(a) and (b), respectively. These spectra have been analyzed on the basis of the Raman markers of polarons and bipolarons obtained from the Raman spectra of the radical anions and the dianions of *p*-oligophenyls.[58] For example, the Raman spectra of the neutral species, the radical anion, and the dianion of *p*-quinquephenyl are shown in Figure 12. The 514.5-nm excited Raman spectrum of Na-doped poly(*p*-phenylene) is attributed to negative polarons, because this spectrum is similar to those of the radical anions of *p*-oligophenyls (Figure 12b). On the other hand, the 1064-nm excited spectrum of Na-doped poly(*p*-phenylene) is ascribed to negative bipolarons, because this spectrum is similar to those of the dianions of *p*-oligophenyls (Figure 12c). Thus, the Raman bands of polarons and bipolarons have been selectively observed by changing the excitation wavelength from 514.5 to 1064 nm. Raman bands arising from the polarons and the bipolarons have been assigned on the basis of the data of ^{13}C-substituted poly(*p*-phenylene).[41] Two significant features in the Raman spectra of polarons and bipolarons are as follows.

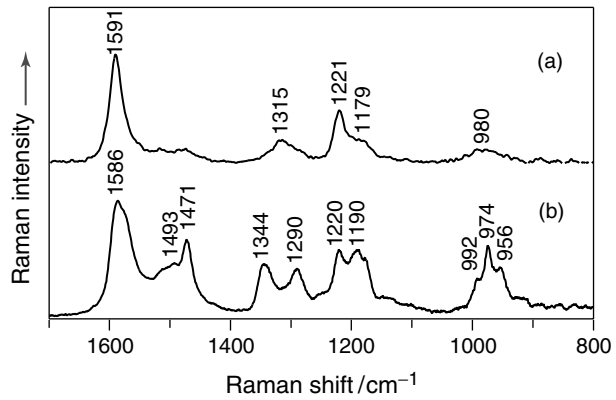

Figure 11. Raman spectra of Na-doped poly(*p*-phenylene). Excitation wavelengths are (a) 514.5 and (b) 1064 nm, respectively.

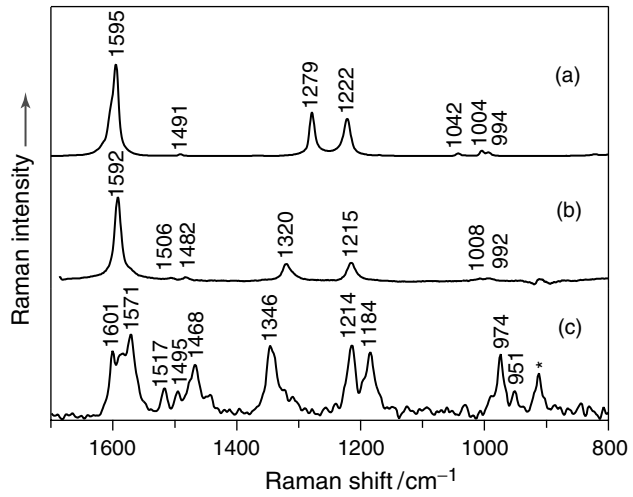

Figure 12. Raman spectra of various oxidation states of *p*-quinquephenyl: (a) neutral species; (b) radical anion; (c) dianion. Excitation wavelengths used in (a), (b), and (c) are 514.5, 514.5, and 1064 nm, respectively. (a) Solid; (b) and (c), THF solutions. The bands of THF are subtracted in (b). The band marked with an asterisk is due to THF. Background due to fluorescence has been subtracted in (c).

1. The wavenumbers of the inter-ring CC stretchings reflect the structures of polarons (radical anions) and bipolarons (dianions). The 1282-cm^{-1} Raman band of pristine poly(*p*-phenylene) (Figure 3c), the 1315-cm^{-1} band due to polarons, and the 1344-cm^{-1} band due to bipolarons are assigned to the inter-ring CC stretchings. The wavenumber of the inter-ring CC stretching shows the 33-cm^{-1} upshift on going from the neutral polymer to polarons and the 62-cm^{-1} upshift on going from the neutral polymer to bipolarons. These observations are explained by changes in the order of the inter-ring CC bonds; that is, the length of the inter-ring CC bonds in the order: neutral species > polaron > bipolaron.
2. The spectral features of the 1064-nm excited Raman spectrum attributed to negative bipolarons are quite different from those of the 514.5-nm excited spectrum attributed to negative polarons. The 1591-, 1315-, and 1221-cm^{-1} bands due to negative polarons can be correlated to the 1595-, 1282-, and 1222-cm^{-1} bands (a_g modes) of the neutral polymer, respectively. Similarly, the 1586-, 1344-, and 1220-cm^{-1} Raman bands due to negative bipolarons can be correlated to the same three bands of the neutral polymer, respectively. The other observed bands of bipolarons originate from Raman-inactive modes of the neutral polymer with D_{2h} symmetry. The appearance of these Raman-inactive modes may be explained by considering that the formation of bipolarons breaks translational symmetry; bipolarons are localized on the several rings of the polymer chain.

3.4 Doped poly(*p*-phenylenevinylene)

Upon doping with sulfuric acid (H_2SO_4), the electronic absorption band of neutral polymer disappears and new absorption bands appear at 2.25 and 1.00 eV (551 and 1240 nm).[59] These two absorptions are due to positive polarons generated by H_2SO_4 doping. Figure 13 shows the Raman spectra of a H_2SO_4-doped poly(*p*-phenylenevinylene) film with various excitation wavelengths (441.6, 514.5, 632.8, 711.0, 740.0, and 1064 nm). The observed

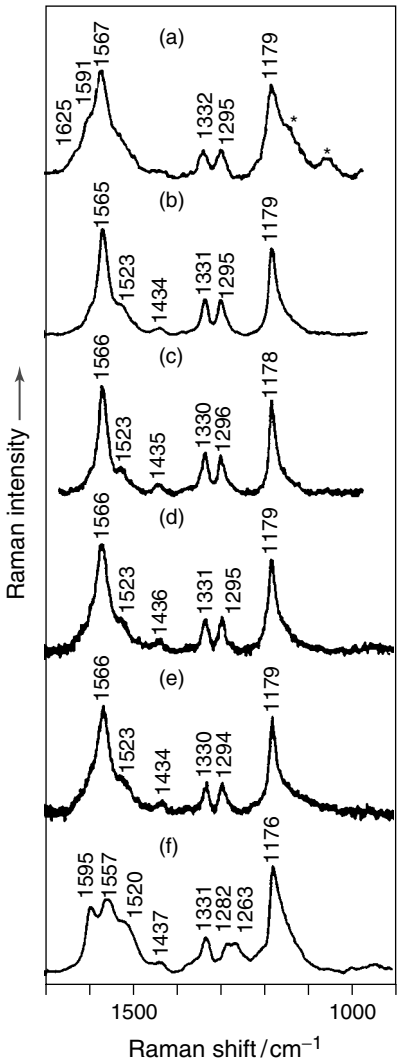

Figure 13. Raman spectra of a H_2SO_4-treated poly(*p*-phenylenevinylene) film. Excitation wavelengths are 441.6, 514.5, 632.8, 711.0, 740.0, and 1064 nm for (a)–(f), respectively. Asterisks indicate the bands of H_2SO_4. Fluorescence backgrounds are subtracted in all the spectra. [Reproduced by permission of American Chemical Society from A. Sakamoto, Y. Furukawa and M. Tasumi, *J. Phys. Chem.*, **98**, 4635 (1994).]

Raman spectra show only small changes with the exciting laser wavelengths 441.6, 514.5, 632.8, 711.0, and 740.0 nm, which locate within the broad band observed at 2.25 eV. The Raman spectra obtained with excitations at 441.6, 514.5, 632.8, 711.0, and 740.0 nm are essentially the same as the Raman spectrum of the radical cation of an oligomer having two vinylene groups and three benzene rings. The radical cation corresponds to a positive polaron. Thus these spectra originate from positive polarons generated by H_2SO_4 doping. The 1064-nm excited Raman spectrum is different from those obtained with other wavelengths, as shown in Figure 13. It has been concluded that this spectrum is contributed by the inter-chain polaron dimers, on the basis of the Raman spectra of the dimer of the radical cations of the model oligomer.[60]

A single electronic absorption band appears at 1.55 eV (800 nm) upon Na doping,[19] which is in contrast to the result of H_2SO_4 doping. This band is attributable to bipolarons, because a bipolaron gives rise to a single sub-gap absorption band. However, different results have been obtained from a Raman study.[61] Figure 14 shows the Raman spectra of a Na-doped poly(*p*-phenylenevinylene) film with various excitation wavelengths (488.0, 514.5, 632.8, 711.0, 740.0, and 1064 nm). The observed Raman spectra strongly depend on excitation wavelength. These spectra have been analyzed on the basis of the Raman spectra of the radical anions and the dianions of three oligomers.

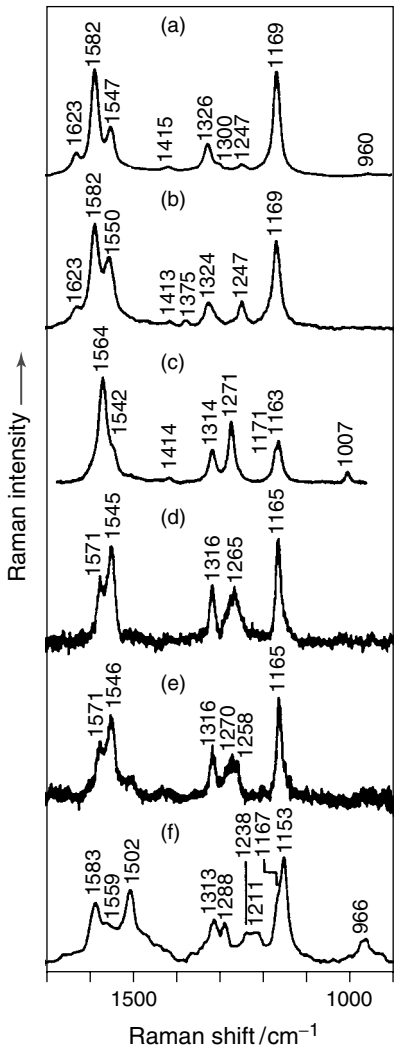

Figure 14. Raman spectra of a Na-doped poly(*p*-phenylenevinylene) film. Excitation wavelengths are 488.0, 514.5, 632.8, 711.0, 740.0, and 1064 nm for (a)–(f), respectively. Fluorescence backgrounds are subtracted in (b), (d), (e), and (f). [Reproduced by permission of American Chemical Society from A. Sakamoto, Y. Furukawa and M. Tasumi, *J. Phys. Chem.*, **96**, 3870 (1992).]

As a result, the observed Raman spectra of Na-doped poly(*p*-phenylenevinylene) have been explained by the coexistence of polarons and bipolarons having various localization lengths. Since each species has its electronic absorption, the Raman bands due to the species is resonantly enhanced by choosing the excitation wavelength within the broad doping-induced absorption band. The major species generated by Na doping is negative bipolarons, because the electronic absorption maximum is observed at 1.55 eV.

4 DOPING- AND PHOTO-INDUCED INFRARED ABSORPTION

The charge carriers in conjugated polymers can be generated by chemical doping and light irradiation. The formation of carriers such as polarons, bipolarons, and charged solitons are associated with structural changes and localized vibrational modes as well as localized electronic states within the band gap. Doping- and photo-induced Infrared active vibrational (IRAV) modes can be observed in the IR region.[62–64] The iodine-doping-induced IR absorption spectra of *trans*-polyacetylene, polythiophene, poly(*p*-phenylene), and MEH-PPV are shown in Figure 15. Photoinduced IR absorption spectra of *trans*-polyacetylene, polythiophene, poly(*p*-phenylene), and poly(*p*-phenylenevinylene) are shown in Figure 16. These spectra were measured at 78 K by the Fourier transform infrared (FT-IR) difference-spectrum method.[65] The absorptivities of the doping- and photo-induced IR bands are far larger than those of pristine polymers. The generated charged species give rise to giant IR intensities. Thus, even if the concentration of carriers is very low, the carriers can be detected by IR spectroscopy. The doping- and photo-induced IR bands as well as the Raman spectra of pristine polymers have been explained successfully in terms of the ECC theory proposed by Zerbi *et al.*[16,18] In their model, charge oscillation along the polymer chain induces strong IR intensities. The vibrational modes corresponding to the totally symmetric modes inducing oscillation in bond alternation for a neutral polymer are strongly observed in the IR spectra due to carriers generated by chemical doping and light irradiation. Thus, the doping- and photo-induced IR bands correspond to the totally symmetric Raman bands of its neutral polymer. However, the number of doping- or photo-induced IR bands is in general larger than that of the totally symmetric modes of the pristine polymer. For example, in the IR spectrum of iodine-doped polythiophene 11 doping-induced bands are observed, although there are 7 a_g modes. It should be noted that the ECC theory is a good approximation method,

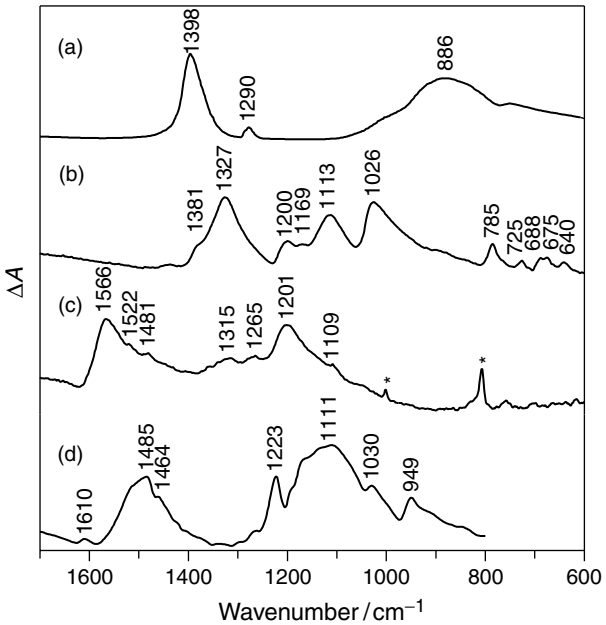

Figure 15. IR absorption spectra of iodine-doped conjugated polymers: (a) *trans*-polyacetylene; (b) polythiophene; (c) poly(*p*-phenylene); (d) MEH-PPV.

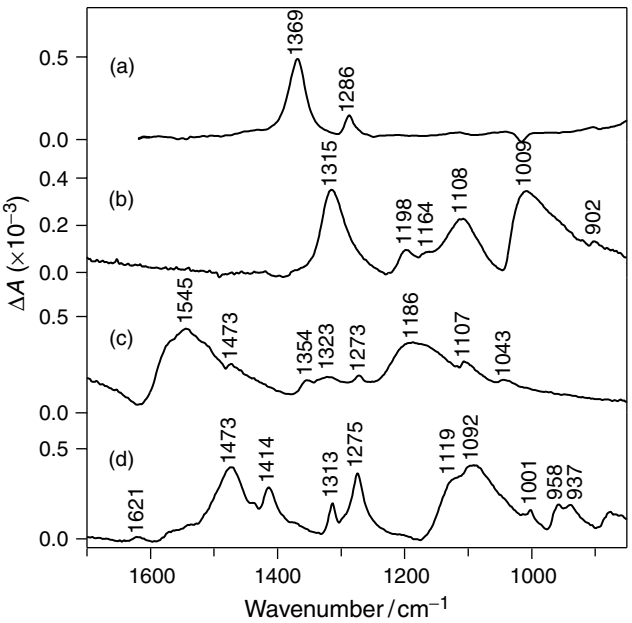

Figure 16. Photoinduced IR absorption spectra of conjugated polymers: (a) *trans*-polyacetylene; (b) polythiophene; (c) poly(*p*-phenylene); (d) poly(*p*-phenylenevinylene). Temperature, 78 K.

but is not complete. It is expected that the normal coordinate calculations based on ab initio molecular orbital methods of the charged oligomers is useful in analyzing doping- and photo-induced IR spectra. We can identify the types of carriers by sub-gap electronic transitions appearing in the region from visible to IR. In the lightly iodine-doped polythiophene, poly(*p*-phenylene), and MEH-PPV,

two sub-gap absorption bands are observed. These two bands are attributable to positive polarons. Therefore, the doping-induced IR bands are ascribed to positive polarons. Similarly, photoinduced IR spectra of polythiophene, poly(*p*-phenylene), and poly(*p*-phenylenevinylene) are also ascribed to polarons generated by light irradiation. On the other hand, in the case of *trans*-polyacetylene having a degenerate ground state, doping- and photo-induced IR absorption spectra are assigned to charged solitons.[62–64] The decay mechanism of photogenerated carriers in the micro- to millisecond region has been studied by means of the phase-modulation technique.[66,67] The observed results have been explained on the basis of the second-order kinetics involving a neutralization recombination process between the positive and negative polarons. The mechanism of carrier generation induced by light irradiation has been studied by picosecond time-resolved IR spectroscopy.[68,69] Moses *et al*.[68] have concluded that carriers are photoexcited directly, and are not generated via excitons. However, carrier generation via excitons has been proposed by Köhler *et al*.[70]

In the composite of a conjugated polymer and C_{60}, electrons are transferred from the conjugated polymer to C_{60} by light irradiation.[71] These composites are promising candidates for photovoltaic cells and solar cells. Ultrafast spectroscopy has shown that the charge separation occurs within a few hundred femtoseconds, with a very slow back transfer. The photoinduced IR absorption spectra of poly(2,5-dioctyloxy-*p*-phenylenevinylene) (DOO-PPV) and DOO-PPV/C_{60} composite measured at 77 K are shown in Figure 17(a) and (b), respectively.[72] Photoinduced spectra are attributed to polarons generated by light irradiation. The intensities of the bands due to polarons are enhanced more than ten times by the addition of C_{60}. The carrier generation has been studied by picosecond time-resolved IR absorption spectroscopy.[73]

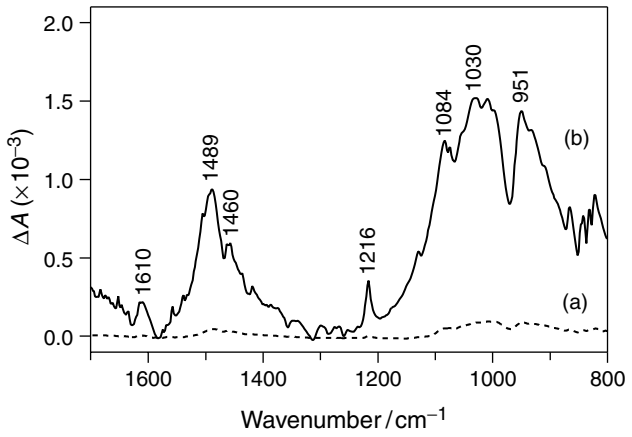

Figure 17. Photoinduced IR absorption spectra of (a) DOO-PPV and (b) DOO-PPV/C_{60} composite. Temperature, 78 K.

5 INFRARED SPECTRA OF INJECTED CARRIERS

The polymer light-emitting diodes fabricated with poly(*p*-phenylenevinylene) derivatives, poly(fluorene) derivatives, etc., show high power efficiencies. The schematic structure of a single-layer polymer light-emitting diode is shown in Figure 18. In the light-emitting diodes fabricated with a conjugated polymer, it is considered that carriers are injected from electrodes to the polymer layer by the application of voltage. The electroluminescence results from the radiative decay of the singlet excitons that are formed by the recombination of injected positive and negative carriers. The information about carriers and/or excitons can be obtained by in situ IR reflective absorption spectroscopy.[74,75] The polymer light-emitting diode was placed on an external reflection apparatus of an FT-IR spectrophotometer. IR light was incident on the BaF_2 plate and reflected off the metal electrode. IR light passed through the polymer layer twice. The reflected IR light was returned to the spectrophotometer. The voltage-induced IR absorption spectra were measured by the FT-IR difference-spectrum method. The voltage-induced IR absorption spectra of the light-emitting diodes fabricated with DOO-PPV and MEH-PPV are shown in Figure 19.[74,75] Since the observed spectrum is similar to that of iodine-doped polymer for each polymer, the observed spectrum probably is attributed to injected positive carriers (polarons); negative carriers are not observed. The observation of the positive carriers is probably related to the predominance of injected positive carriers in these polymer light-emitting diodes.[75] In order to make more efficient light-emitting diodes, the injection of more negative carriers is required.

6 CONCLUDING REMARKS

It has been demonstrated that IR and Raman spectroscopy is a powerful tool for studying the structures of doped as well as pristine conjugated polymers. The charge carriers such as charged solitons, polarons, and bipolarons can be generated

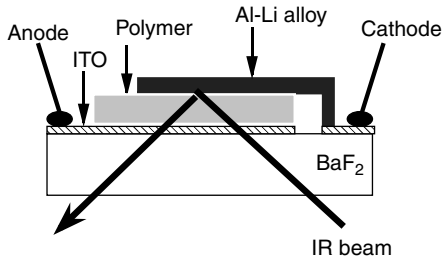

Figure 18. Schematic structure of a single-layer light-emitting diode fabricated with a conjugated polymer.

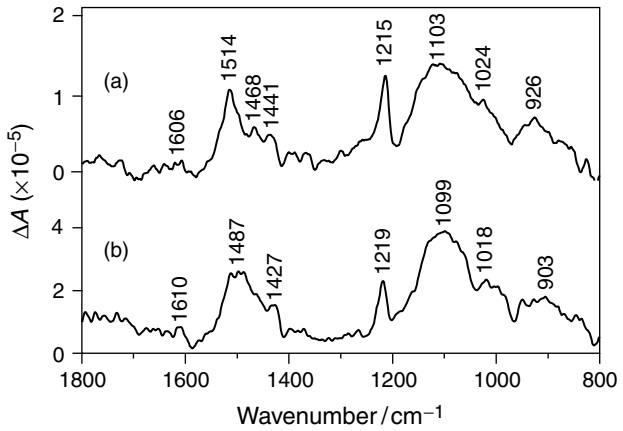

Figure 19. Voltage-induced IR reflective absorption spectra of the light-emitting diodes fabricated with (a) DOO-PPV and (b) MEH-PPV at room temperature.

by doping. Polarons and bipolarons generated by chemical doping have been identified by Raman spectroscopy. IR spectroscopy is a powerful tool for detecting the photogenerated and injected carriers in polymer optoelectronic devices, because the carriers give rise to giant IR intensities. In situ IR spectroscopy will be useful in studies of light-emitting diodes, solar cells, and field-effect transistors fabricated with conjugated polymers.

ABBREVIATIONS AND ACRONYMS

DOO-PPV	Poly(2,5-dioctyloxy-*p*-phenylenevinylene)
ECC	Effective Conjugation Coordinate
IRAV	Infrared Active Vibrational
MEH-PPV	Poly(2-methoxy-5-(2′-ethylhexyloxy)-*p*-phenylenevinylene)
THF	Tetrahydrofuran
TNBC	19,19′,20,20′-Tetranor-β,β-carotene

REFERENCES

1. T.A. Skotheim, R.L. Elsenbaumer and J.R. Reynolds (eds), 'Handbook of Conducting Polymers', Marcel Dekker, New York (1997).
2. N.S. Sariciftci (ed.), 'Primary Photoexcitations in Conjugated Polymers: Molecular Exciton versus Semiconductor Band Model', World Scientific, Singapore (1997).
3. H. Kiess (ed.), 'Conjugated Conducting Polymers', Springer-Verlag, Berlin (1992).
4. A. Tsumura, H. Koezuka and T. Ando, *Appl. Phys. Lett.*, **49**, 1210 (1986).
5. J.H. Burroughes, C.A. Jones and R.H. Friend, *Nature*, **335**, 137 (1988).
6. G. Yu, J. Gao, J.C. Hummelen, F. Wudl and A.J. Heeger, *Science*, **270**, 1789 (1995).
7. J.H. Burroughes, D.D.C. Bradley, A.R. Brown, R.N. Marks, K. Mackay, R.H. Friend, P.L. Burns and A.B. Holmes, *Nature*, **347**, 539 (1990).
8. R.H. Friend, R.W. Gymer, A.B. Holmes, J.H. Burroughes, R.N. Marks, C. Taliani, D.D.C. Bradley, D.A. Dos Santos, J.L. Brédas, M. Lögdlund and W.R. Salaneck, *Nature*, **397**, 121 (1999).
9. W.P. Su, J.R. Schrieffer and A.J. Heeger, *Phys. Rev. B*, **22**, 2099 (1980).
10. W.P. Su and J.R. Schrieffer, *Proc. Natl. Acad. Sci. USA*, **77**, 5626 (1980).
11. S.A. Brazovskiĭ and N.N. Kirova, *Sov. Phys. JETP Lett.*, **33**, 4 (1981).
12. A.R. Bishop, D.K. Campbell and K. Fesser, *Mol. Cryst. Liq. Cryst.*, **77**, 253 (1981).
13. J.L. Brédas, R.R. Chance and R. Silbey, *Mol. Cryst. Liq. Cryst.*, **77**, 319 (1981).
14. H. Kuzmany, *Makromol. Chem., Makromol. Symp.*, **37**, 81 (1990).
15. I. Harada and Y. Furukawa, 'Vibrational Spectra and Structure of Conjugated and Conducting Polymers', in "Vibrational Spectra and Structure", ed. J.R. Durig, Elsevier, Amsterdam, 369–469, Vol. 19 (1991).
16. M. Gussoni, C. Castiglioni and G. Zerbi, 'Vibrational Spectroscopy of Polyconjugated Materials: Polyacetylene and Polyenes', in "Spectroscopy of Advanced Materials", eds R.J.H. Clark and R.E. Hester, John Wiley & Sons, Chichester, 251–353 (1991).
17. A.J. Epstein, R.P. McCall, J.M. Ginder and A.G. MacDiarmid, 'Spectroscopy and Photoexcitation Spectroscopy of Polyaniline: A Model System for New Phenomena', in "Spectroscopy of Advanced Materials", eds R.J.H. Clark and R.E. Hester, John Wiley & Sons, Chichester, 355–396 (1991).
18. G. Zerbi, M. Gussoni and C. Castiglioni, 'Vibrational Spectroscopy of Polyconjugated Aromatic Materials with Electrical and Nonlinear Optical Properties. A Guided Tour', in "Conjugated Polymers", eds J.L. Brédas and R. Silbey, Kluwer Academic, Dordrecht, 435–507 (1991).
19. Y. Furukawa, A. Sakamoto and M. Tasumi, *Macromol. Symp.*, **101**, 95 (1996).
20. Y. Furukawa, *J. Phys. Chem.*, **100**, 15 644 (1996).
21. Y. Furukawa and M. Tasumi, 'Vibrational Spectroscopy of Intact and Doped Conjugated Polymers and Their Models', in "Modern Polymer Spectroscopy", ed. G. Zerbi, Wiley-VCH, Weinheim, 207–237 (1991).
22. H. Shirakawa and S. Ikeda, *Polymer J.*, **2**, 231 (1971).
23. H. Kuzmany, *Phys. Status Solidi B*, **97**, 521 (1980).
24. G. Zannoni and G. Zerbi, *J. Mol. Struct.*, **100**, 485 (1983).
25. D. Jumeau, S. Lefrant, E. Faulques and J.P. Buisson, *J. Physique*, **44**, 819 (1983).
26. H. Takeuchi, T. Arakawa, Y. Furukawa, I. Harada and H. Shirakawa, *J. Mol. Struct.*, **158**, 179 (1987).

27. S. Hirata, H. Torii and M. Tasumi, *J. Chem. Phys.*, **103**, 8964 (1995).
28. C. Castiglioni, J.T.L. Navarrete, G. Zerbi and M. Gussoni, *Solid State Commun.*, **65**, 625 (1988).
29. B. Horovitz, *Solid State Commun.*, **41**, 729 (1982).
30. E. Ehrenfreund, Z. Vardeny, O. Brafman and B. Horovitz, *Phys. Rev. B*, **36**, 1535 (1987).
31. K. Akagi, G. Piao, S. Kaneko, K. Sakamaki, H. Shirakawa and M. Kyotani, *Science*, **282**, 1683 (1998).
32. G. Poussigue and C. Benoit, *J. Phys. Condens. Matter*, **1**, 9547 (1989).
33. E. Faulques, W. Wallnöfer and H. Kuzmany, *J. Chem. Phys.*, **90**, 7585 (1989).
34. C.X. Cui, M. Kertesz and H. Eckhardt, *Synth. Met.*, **43**, 3491 (1991).
35. J.T.L. Navarrete and G. Zerbi, *J. Chem. Phys.*, **94**, 957 (1991).
36. M. Kofranek, T. Kovár, H. Lischka and A. Karpfen, *J. Mol. Struct. (Theochem.)*, **259**, 181 (1992).
37. G. Louarn, J.-Y. Mevellec, J.P. Buisson and S. Lefrant, *Synth. Met.*, **55**, 587 (1993).
38. G. Zannoni and G. Zerbi, *J. Chem. Phys.*, **82**, 31 (1985).
39. K. Krichene, J.P. Buisson and S. Lefrant, *Synth. Met.*, **17**, 589 (1987).
40. L. Cuff and M. Kertesz, *Macromolecules*, **27**, 762 (1994).
41. Y. Furukawa, H. Ohtsuka, M. Tasumi, I. Wataru, T. Kanbara and T. Yamamoto, *J. Raman Spectrosc.*, **24**, 551 (1993).
42. B. Tian and G. Zerbi, *J. Chem. Phys.*, **95**, 3198 (1991).
43. I. Orion, J.P. Buisson and S. Lefrant, *Phys. Rev. B*, **57**, 7050 (1998).
44. Y. Furukawa, A. Sakamoto, H. Ohta and M. Tasumi, *Synth. Met.*, **49**, 335 (1992).
45. Y. Furukawa, *Synth. Met.*, **69**, 629 (1995).
46. I. Harada, Y. Furukawa, M. Tasumi and H. Shirakawa, *J. Chem. Phys.*, **73**, 4746 (1980).
47. J. Tanaka, Y. Saito, M. Shimizu, C. Tanaka and M. Tanaka, *Bull. Chem. Soc. Jpn.*, **60**, 1595 (1987).
48. Y. Furukawa, H. Ohta, A. Sakamoto and M. Tasumi, *Spectrochim. Acta*, **47A**, 1367 (1991).
49. S. Lefrant, E. Mulazzi and C. Mathis, *Phys. Rev. B*, **49**, 13 400 (1994).
50. J.-Y. Kim, S. Ando, A. Sakamoto, Y. Furukawa and M. Tasumi, *Synth. Met.*, **89**, 149 (1997).
51. J.-Y. Kim, Y. Furukawa and M. Tasumi, *Chem. Phys. Lett.*, **276**, 418 (1997).
52. Y. Kawashima, K. Nakayama, H. Nakano and K. Hirao, *Chem. Phys. Lett.*, **267**, 82 (1997).
53. N. Yokonuma, Y. Furukawa, M. Tasumi, M. Kuroda and J. Nakayama, *Chem. Phys. Lett.*, **255**, 431 (1996).
54. Ch. Ehrendorfer and A. Karpfen, *Vib. Spectrosc.*, **8**, 293 (1995).
55. Ch. Ehrendorfer and A. Karpfen, *J. Phys. Chem.*, **99**, 5341 (1995).
56. J. Casado, V. Hernández, S. Hotta and J.T.L. Navarrete, *J. Chem. Phys.*, **109**, 10 419 (1998).
57. J.J. Apperloo, J.A.E.H. van Haare and R.A.J. Janssen, *Synth. Met.*, **101**, 417 (1999).
58. Y. Furukawa, H. Ohtsuka and M. Tasumi, *Synth. Met.*, **55**, 516 (1993).
59. A. Sakamoto, Y. Furukawa and M. Tasumi, *J. Phys. Chem.*, **98**, 4635 (1994).
60. A. Sakamoto, Y. Furukawa and M. Tasumi, *J. Phys. Chem.*, **101**, 1726 (1997).
61. A. Sakamoto, Y. Furukawa and M. Tasumi, *J. Phys. Chem.*, **96**, 3870 (1992).
62. C.R. Fincher, Jr, M. Ozaki, A.J. Heeger and A.G. MacDiarmid, *Phys. Rev. B*, **19**, 4140 (1979).
63. Z. Vardeny, J. Orenstein and G.L. Baker, *Phys. Rev. Lett.*, **50**, 2032 (1983).
64. G.B. Blanchet, C.R. Fincher, T.C. Chung and A.J. Heeger, *Phys. Rev. Lett.*, **50**, 1938 (1983).
65. Y.-H. Cha, Y. Furukawa, M. Tasumi, T. Noguchi and T. Ohnishi, *Chem. Phys. Lett.*, **273**, 159 (1997).
66. Y. Furukawa, *Appl. Spectrosc.*, **47**, 1405 (1993).
67. Y. Furukawa, Y.-H. Cha, T. Noguchi, T. Ohnishi and M. Tasumi, *J. Mol. Struct.*, **521**, 211 (2000).
68. D. Moses, A. Dogariu and A.J. Heeger, *Chem. Phys. Lett.*, **316**, 356 (2000).
69. A. Sakamoto, O. Nakamura, G. Yoshimoto and M. Tasumi, *J. Phys. Chem. A*, **104**, 4198 (2000).
70. A. Köhler, D.A. dos Santos, D. Beljonne, Z. Shuai, J.-L. Brédas, A.B. Holmes, A. Kraus, K. Müllen and R.H. Friend, *Nature*, **392**, 903 (1998).
71. N.S. Sariciftci, *Prog. Quant. Electr.*, **19**, 131 (1995).
72. K. Kudo and Y. Furukawa, Personal communication.
73. U. Mizrahi, I. Shtrichman, D. Gershoni, E. Ehrenfreund and Z.V. Vardeny, *Synth. Met.*, **102**, 1182 (1999).
74. M. Ishima, Y. Furukawa, T. Noguchi and T. Ohnishi, 'Infrared Spectra of the Electroluminescent Devices Based on Poly(2,5-dioctyloxy-*p*-phenylenevinylene', in "Proceedings of the Twelfth International Conference on Fourier Transform Spectroscopy", eds K. Itoh and M. Tasumi, Waseda University Press, Tokyo, 423–424 (1999).
75. Y. Furukawa, M. Ishima, T. Noguchi and T. Ohnishi, *Synth. Met.*, in press.